University of Sistan and Baluchestan

Chemical Process Design

Available online at http://cpd.usb.ac.ir/




# Thermal Degradation Kinetics of Cellulose: Mechanisms and Implications for Sustainable Energy

Bahador Abolpour[1], Hanie Abbaslou[2]✉

[1] Department of Chemical Engineering, Sirjan University of Technology, Sirjan, Iran. Email: Bahadorabolpor1364@sirjantech.ac.ir. https://orcid.org/0000-0002-9403-6359
[2] Corresponding Author, Department of Environment and Civil Engineering, Sirjan University of Technology, Sirjan, Iran. Email: abbslou@sirjantech.ac.ir. https://orcid.org/0000-0002-4675-7389

## ARTICLE INFO

***Article type:***
*Research Article*

***Article history:***
*Received: 2025-12-02*
*Received in revised form: 2026-04-20*
*Accepted: 2026-07-12*
*Available online: 2026-07-12*

***Keywords:*** *Cellulose, Thermal decomposition; Kinetics; Thermo-gravimetric; Diffusion Model*

## ABSTRACT

Cellulose is a key constituent of biomass and an important material for sustainable energy and fire-safe applications. Despite extensive studies on cellulose pyrolysis, the dominant degradation mechanism under strictly isothermal conditions remains insufficiently clarified. In this work, the thermal degradation kinetics of cellulose were systematically investigated using isothermal thermogravimetric analysis (TGA) within a narrow temperature range of 580–610 K. Both model-fitting and iso-conversional (model-free) approaches were employed to determine kinetic parameters and identify the governing reaction mechanism. The results demonstrate that cellulose degradation is predominantly governed by geometric contraction mechanisms, specifically contracting area and contracting volume models, indicating that the reaction rate is controlled by progressive reduction of the reactive interface. Power-law behavior with exponents of 1/2 and 1/3 was observed at the early stages of conversion, while nucleation and diffusion models showed limited applicability. The apparent activation energy was determined to be in the range of 1.75–2.79 × $10^8$ J·kmol$^{-1}$, indicating a relatively low energy barrier for cellulose decomposition under isothermal conditions. The novelty of this study lies in the combination of strictly isothermal analysis, narrow temperature control, and comprehensive comparison of solid-state kinetic models, enabling clear identification of the dominant degradation mechanism. A predictive kinetic equation for cellulose degradation was developed, providing useful insights for reactor design, biomass conversion, and flame-retardant material development.

**Cite this article:** Abolpour, B., Abbaslou, H., (2027) Thermal Degradation Kinetics of Cellulose: Mechanisms and Implications for Sustainable Energy, *Chemical Process Design*, 6(1), 1-14. http//doi.org/10.22111/cpd.2026.54070.1081

© The Author(s).
DOI: http//doi.org/10.22111/cpd.2026.54070.1081

Publisher: University of Sistan and Baluchestan.

ARTICLE IN PRESS

## 1. Introduction

Understanding the thermal degradation pathways of cellulose is essential for advancing its use in renewable energy and materials science. As a primary component of biomass, cellulose serves as a potential fuel source, and its decomposition behavior directly impacts combustion efficiency and product formation [1, 2]. Additionally, the thermal stability and flame-retardant characteristics of cellulosic materials are vital for mitigating fire risks and reducing emissions of harmful compounds during processes like waste incineration or resource recovery from lignocellulosic waste [3, 4].

These materials also play a vital role in optimizing incineration processes and minimizing energy production from fossil fuels, along with the pollution that accompanies it. Additionally, cellulose is recognized as an innovative polymer derived from renewable resources. The thermal degradation process is pivotal as it influences the rate at which various products from cellulosic materials are generated, which is essential for the aforementioned applications.

Isothermal analysis methods provide distinct advantages for studying decomposition kinetics. First, conducting measurements at constant temperature allows for the direct derivation of reaction rates, making it easier to identify shifts in reaction mechanisms or order. Second, the rate constants can often be obtained from straightforward analytical solutions, simplifying parameter estimation. Finally, once thermal equilibrium is achieved, the sample temperature becomes uniform, eliminating the internal temperature gradients that can complicate the interpretation of dynamic (non-isothermal) TGA data [5].

Given that the processing temperatures for thermoplastics frequently surpass 400 K, the thermal stability of cellulose emerges as a crucial determinant in its efficacy as a reinforcement material [6]. Numerous studies have been conducted to ascertain the thermal characteristics of cellulose, including its glass transition temperatures and the melting points of cellulose esters [7, 8, 9]. Research by Huang and Li [10] focused on the thermal stability of cellulose, while Jandura et al. [9] and Huang [11] delved into the kinetics of thermal degradation of cellulose. Additionally, Dahiya et al. [12] proposed a comparable methodology for determining the degradation kinetics of cellulose. Therefore, a detailed investigation into the specific degradation mechanism of cellulose and the accurate determination of its kinetic parameters is necessary. This study applies established solid-state reaction analysis techniques to achieve this goal. The primary objective is to elucidate the thermal degradation mechanism of cellulose and obtain the corresponding kinetic parameters within the 580–610 K temperature range. Special care was taken in the experimental design to minimize potential diffusion limitations, ensuring the observed kinetics reflect the intrinsic chemical process.

Recent studies have significantly advanced the understanding of cellulose thermal degradation through improved kinetic modeling, advanced data processing techniques, and coupling of experimental and numerical approaches. Li et al. [13] employed iso-conversional and distributed activation energy models to analyze cellulose pyrolysis under inert atmospheres, emphasizing the influence of temperature programs on apparent activation energy distributions. Similarly, Wang et al. [14] investigated the effect of particle size and crystallinity on cellulose degradation kinetics, reporting that surface-controlled mechanisms become dominant for finely divided cellulose samples. Zhao et al. [15] applied combined TGA–FTIR techniques to elucidate the evolution of gaseous products during cellulose decomposition, highlighting the importance of reaction interfaces in controlling degradation rates. Moreover, Martínez et al. [16] compared isothermal and non-isothermal kinetic analyses and concluded that isothermal methods

ARTICLE IN PRESS

provide more reliable mechanistic interpretations when diffusion limitations are minimized. A recent review by Kim and Park [17] summarized advances in biomass kinetic modeling and emphasized the growing need for mechanism-oriented studies rather than sole reliance on activation energy estimation. Despite these advances, the dominant solid-state mechanism governing cellulose degradation under strictly isothermal conditions remains insufficiently addressed, particularly within narrow temperature ranges relevant to industrial processing. The present study directly addresses this gap.

Although the thermal degradation of cellulose has been extensively studied, most existing investigations rely on non-isothermal thermogravimetric analysis, wide temperature ranges, or distributed activation energy models. Under such conditions, overlapping reactions, internal temperature gradients, and diffusion effects may obscure the intrinsic degradation mechanism. Furthermore, many studies focus primarily on determining activation energy values rather than identifying the dominant solid-state reaction mechanism governing cellulose decomposition.

In particular, strictly isothermal kinetic analyses conducted within a narrow temperature window are scarce, despite their importance for isolating chemical reaction control from heat and mass transfer limitations. The lack of consensus regarding whether cellulose degradation is governed by nucleation, diffusion, reaction-order, or geometrical contraction mechanisms highlights the need for a systematic and controlled mechanistic investigation. The novelty of the present work is threefold: (i) it employs strictly isothermal TGA experiments within a narrow temperature range (580–610 K), minimizing thermal gradients and diffusion limitations; (ii) it performs a comprehensive comparison of multiple solid-state kinetic models, including power-law, nucleation, diffusion, and geometric contraction models, under identical experimental conditions; and (iii) it demonstrates that geometric contraction mechanisms dominate cellulose degradation, enabling the development of a reliable predictive kinetic equation suitable for energy conversion and material design applications.

## 2. Experiments

The cellulose powder under investigation was sourced from CDH, India, exhibiting a precise size distribution within the micron range, with an average particle size of 150 µm. The Argon gas utilized in the experiments was procured from Air-product Company, characterized by its exceptional purity of 99.999%, thereby reducing the potential influence of gas phase impurities on the reaction outcomes.

For this research, a Thermogravimetric Analysis (TGA) system was developed. A tube furnace rated at 3 kW, featuring a heating zone of 40 cm and capable of reaching temperatures up to 1400 K, was constructed. Within this furnace, a vertical ceramic tube with outer and inner diameters of 50 mm and 34 mm, respectively, was installed to serve as the reactor. The crucible, which contained a sample weighing 10 mg, was suspended using a nickel-chrome wire connected to a digital balance (A&D-GF300, with an accuracy of 1 mg) to facilitate precise measurement of the sample's weight within the system. The fluctuations in weight of the crucible's contents were continuously monitored and recorded by a computer linked to the digital balance.

An inert gas stream, specifically Argon, was utilized to safeguard the balance and eliminate the air content within the system. A gas flow meter was employed to accurately measure the volumetric flow rate of this Argon gas. The exhaust gases from the system were directed through a bubbler, which ensured the maintenance of positive pressure within the system. This partial positive pressure serves to mitigate the risk of air ingress in the event of a leak, thereby reducing the potential for explosion. As the system temperature approached the target of approximately 600 K, the Argon stream effectively purged the air from both the ceramic system and the associated tubes. Once the target temperature was

ARTICLE IN PRESS

stabilized, a flow rate of 100 ml/min was introduced from the top of the system, following precise measurement by the volumetric flow meter. The exhaust gases were expelled from the bottom of the system and passed through a bubbler to maintain the positive pressure. Additionally, the weight variation of the concentrate within the crucible was monitored by a computer linked to a digital scale, recording data at one-second intervals.

The following assumptions were adopted to ensure reliable kinetic analysis:

• The sample temperature was assumed to be uniform after an initial stabilization period of 10–15 min at the target isothermal temperature.

• The cellulose particles were sufficiently small (average size ≈150 μm) to neglect internal heat and mass transfer limitations.

• The degradation process was assumed to be dominated by a single overall reaction mechanism within the studied conversion range.

• The argon atmosphere (99.999% purity) ensured inert conditions, preventing oxidative degradation.

• Particle geometry was assumed to remain constant during degradation for the purpose of applying geometric contraction models.

The extent of conversion, x, was calculated using the standard relation:

$$x = \frac{m0-mt}{m0-mf} \quad (1)$$

Where $m_0$, $m_t$, and $m_f$ represent the initial, instantaneous, and final sample masses, respectively.

Each experiment was repeated at least twice to confirm reproducibility, and deviations in mass measurements were within the balance accuracy (±1 mg).

## 3. Mechanisms

The kinetic analysis of cellulose thermal degradation in this work is based on the fundamental rate equation for solid-state reactions. For an isothermal process, the extent of conversion, 'x', as a function of time, 't', can be described by:

$$\frac{dx}{dt} = kf(x) \quad (2)$$

or its differential form:

$$g(x) = kt \quad (3)$$

Here, g(x) and f(x) represent the integral and differential forms of the reaction model, respectively. The rate constant, 'k', is temperature-dependent and follows the Arrhenius law: $k0\exp\left(\frac{-E}{RT}\right)$, where E is the apparent activation energy and R is the universal gas constant. The function g(x) can manifest in various forms, several of which are illustrated in Table 1 [18, 19, 20]. A prevalent approach to analyzing mechanisms of such phenomena involves fitting experimental data, specifically the conversion over time at a constant temperature, to established models, followed by an assessment of this fit through the correlation coefficient ($R^2$) [21].

ARTICLE IN PRESS

The activation energy for degradation can be determined using the Model Free method, which is dependent on the solid conversion rate. By substituting the Arrhenius equation for k into equation (1) and rearranging it into a logarithmic format, we arrive at the essential equation governing the Model Free method under isothermal conditions [19, 22]:

$$-Ln(tx) = Ln\left(\frac{k0}{g(x)}\right) - \frac{Ex}{RT} \quad (4)$$

## 4. Results and Discussions

Figures 1 to 6 demonstrate how the models presented in Table 1 correspond with the experimental data on cellulose degradation under different temperature conditions. Table 1 presents the various solid-state reaction models used to interpret the thermal degradation of cellulose. The models include power-law, Avrami-Erofe'ev, geometric contraction, diffusion, and reaction-order models, with their corresponding mean correlation coefficients ($R^2$ values) averaged over all investigated temperatures. These $R^2$ values are critical as they reflect the degree of fit between the experimental data and the theoretical models. It should be noted that the $R^2$ values reported in Figures 1–6 correspond to temperature-specific fittings, whereas Table 1 presents mean $R^2$ values averaged over the entire investigated temperature range. Minor discrepancies between individual figure values and Table 1 arise from this averaging procedure. This distinction has been clarified to avoid misinterpretation of model performance. The values of k, derived from fitting each model to the experimental data, along with their corresponding $R^2$ values, are illustrated in the Figures provided. Furthermore, the calculated k values in relation to temperature are depicted on the right side of these Figures (1-6), accompanied by the fitted curves based on the Arrhenius equation, which are instrumental in determining the activation energy (E) for the respective models. Models deemed less significant exhibit lower mean $R^2$ values in relation to the determination of k and E. Table 1 offers a comparative analysis of the mean $R^2$ values of the fitted models, where values approaching 1 signify a higher degree of model acceptability for the observed phenomenon. It is important to highlight that the nucleation and growth model incorporates an additional variable compared to the other models, specifically n, which represents the extent of progress in the solid conversion process. Consequently, this dependency is first established (as shown in the left section of Figure 3), and subsequently, the modal value of this variable is utilized to derive k, as illustrated in the central section of the same Figure.

**Table 1.** The common models for understanding the processes involved in the degradation of cellulose.

| Number | Model | *f(X)* | *g(X)* | $R^2_{mean}$ |
|---|---|---|---|---|
| *Nucleation models* | | | | |
| | Power law | | | |
| 1 | | $\frac{2}{3}X^{-\frac{1}{2}}$ | $X^{\frac{3}{2}}$ | 0.928 |
| 2 | | $2X^{\frac{1}{2}}$ | $X^{\frac{1}{2}}$ | 0.775 |
| 3 | | $3X^{\frac{2}{3}}$ | $X^{\frac{1}{3}}$ | 0.705 |
| 4 | | $4X^{\frac{3}{4}}$ | $X^{\frac{1}{4}}$ | 0.661 |
| | Avrami-Erofe'ev | | | |
| 5 | | $\frac{3}{2}(1-X)\left[-\ln(1-X)\right]^{\frac{1}{3}}$ | $\left[-\ln(1-X)\right]^{\frac{2}{3}}$ | 0.848 |
| 6 | | $2(1-X)\left[-\ln(1-X)\right]^{\frac{1}{2}}$ | $\left[-\ln(1-X)\right]^{\frac{1}{2}}$ | 0.915 |
| 7 | | $3(1-X)\left[-\ln(1-X)\right]^{\frac{2}{3}}$ | $\left[-\ln(1-X)\right]^{\frac{1}{3}}$ | 0.882 |
| 8 | | $4(1-X)\left[-\ln(1-X)\right]^{\frac{3}{4}}$ | $\left[-\ln(1-X)\right]^{\frac{1}{4}}$ | 0.821 |

ARTICLE IN PRESS

| | | | | |
|---|---|---|---|---|
| 9 | Nucleation and growth | $n(1-X)\left[-\ln(1-X)\right]^{1-\frac{1}{n}}$ | $\left[-\ln(1-X)\right]^{\frac{1}{n}}$ | 0.917 |
| *Geometrical contraction models* | | | | |
| 10 | Contracting area | $2(1-X)^{\frac{1}{2}}$ | $1-(1-X)^{\frac{1}{2}}$ | **0.955** |
| 11 | Contracting volume | $3(1-X)^{\frac{2}{3}}$ | $1-(1-X)^{\frac{1}{3}}$ | **0.957** |
| *Diffusion models* | | | | |
| 12 | 1D diffusion | $(2X)^{-1}$ | $X^2$ | 0.933 |
| 13 | 2D diffusion | $\left[-\ln(1-X)\right]^{-1}$ | $(1-X)\ln(1-X)+X$ | 0.928 |
| 14 | 3D diffusion | $\frac{3}{2}(1-X)^{\frac{2}{3}}\left[1-(1-X)^{\frac{1}{3}}\right]^{-1}$ | $\left[1-(1-X)^{\frac{1}{3}}\right]^2$ | 0.777 |
| 15 | Ginstling-Brounshtein | $\frac{3}{2}\left[(1-X)^{-\frac{1}{3}}-1\right]^{-1}$ | $1-\frac{2}{3}X-(1-X)^{\frac{2}{3}}$ | 0.91 |
| *Reaction-order models* | | | | |
| 16 | Zero-order | 1 | $X$ | 0.889 |
| 17 | First-order | $(1-X)$ | $-\ln(1-X)$ | 0.562 |
| 18 | Second-order | $(1-X)^2$ | $(1-X)^{-1}-1$ | -0.292 |
| 19 | Third-order | $(1-X)^3$ | $\frac{1}{2}\left[(1-X)^{-2}-1\right]$ | -0.292 |

*Mean correlation coefficients ($R^2$) averaged over all investigated temperatures.*

The geometric contraction models, specifically contracting area and volume, exhibit the highest mean $R^2$ values (0.955 and 0.957, respectively), indicating a superior fit. This suggests that the geometric contraction models are the most appropriate for describing the degradation kinetics of cellulose under the studied conditions. Models such as the power law and diffusion models also demonstrate relatively high $R^2$ values, showing their effectiveness at different stages or aspects of the reaction. The observed high correlation for geometric contraction models supports the hypothesis that the reaction is predominantly surface-controlled, with cellulose particles exhibiting behavior akin to shrinking geometries like cylinders or spheres. This insight can be vital for optimizing industrial processes involving cellulose thermal degradation.

The experimental data can be interpreted using multiple solid-state reaction models. Based on the comparison of mean $R^2$ values in Table 1, the thermal degradation of cellulose in this study is best described by geometric contraction models. In these models, reaction initiation (nucleation) is assumed to occur rapidly at the particle surface. The subsequent reaction front then progresses inwards towards the particle core, with the reaction rate controlled by this moving interface. The contracting area model typically applies to geometries like cylinders, where the interface area decreases in two dimensions, while the contracting volume model is more representative of spheres or cubes, where the reaction front recedes in three dimensions [23]. Given that the cellulose particles utilized in this study lack defined and regular geometries, the $R^2_{mean}$ values calculated for both models are comparable.

ARTICLE IN PRESS

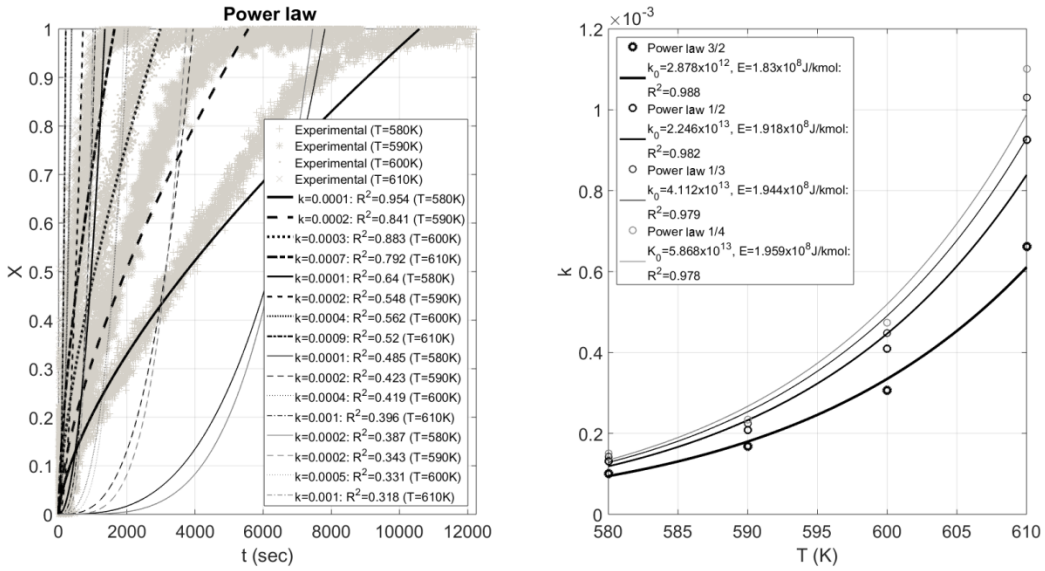



**Figure 1.** The alignment of the power law models with experimental data at different temperatures, along with fitted curves for the rate constant (k), follows the principles of the Arrhenius equation.

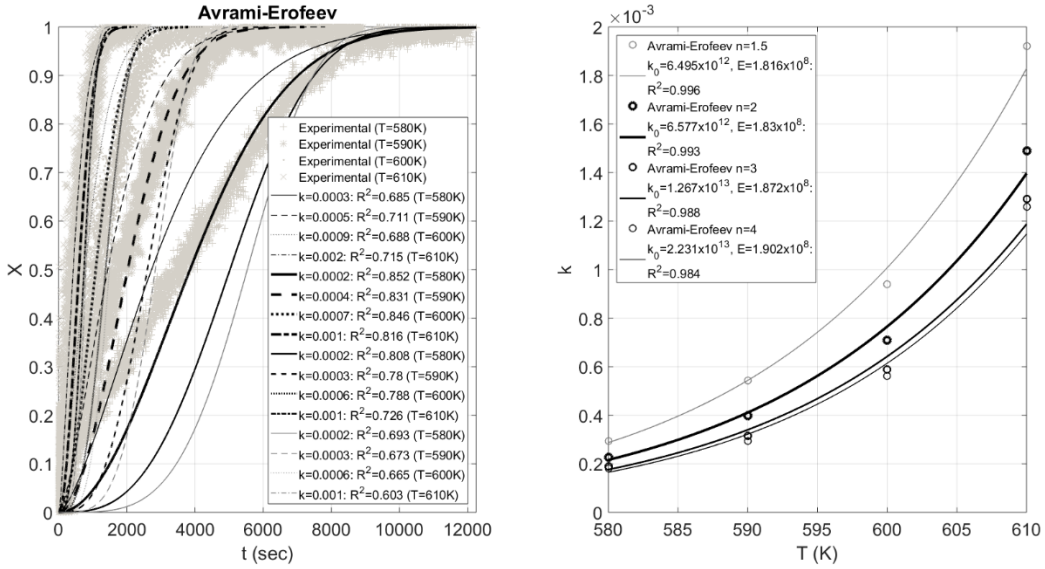



**Figure 2.** The alignment of the Avrami Erofe'ev models with experimental data at different temperatures, along with fitted curves for the rate constant (k), follows the principles of the Arrhenius equation.

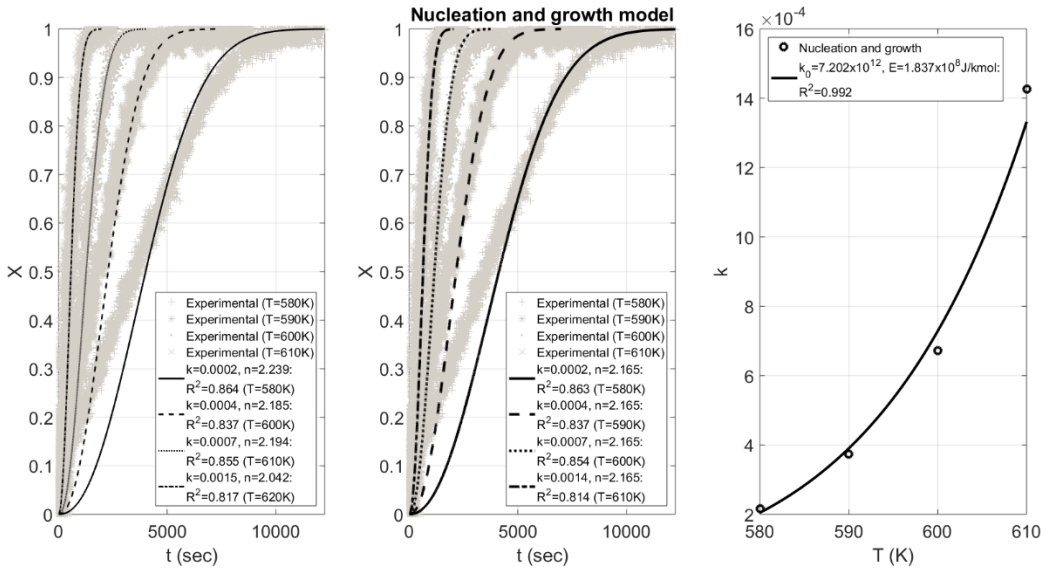



**Figure 3.** The alignment of nucleation and growth models with experimental data at different temperatures, along with fitted curves for the rate constant (k), follows the principles of the Arrhenius equation.

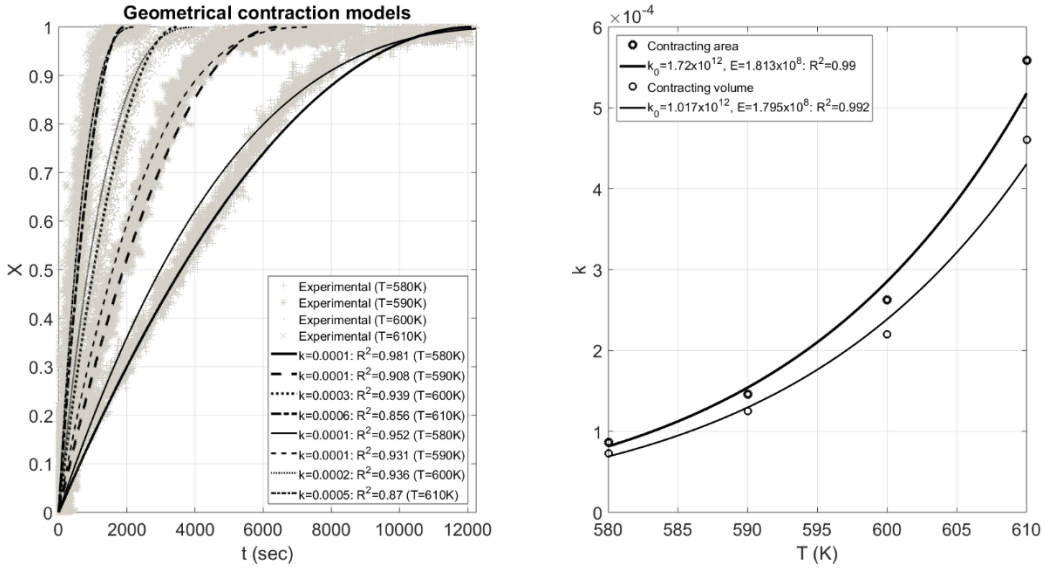



**Figure 4.** The alignment of geometric contraction models with experimental data at different temperatures, along with fitted curves for the rate constant (k), follows the principles of the Arrhenius equation.

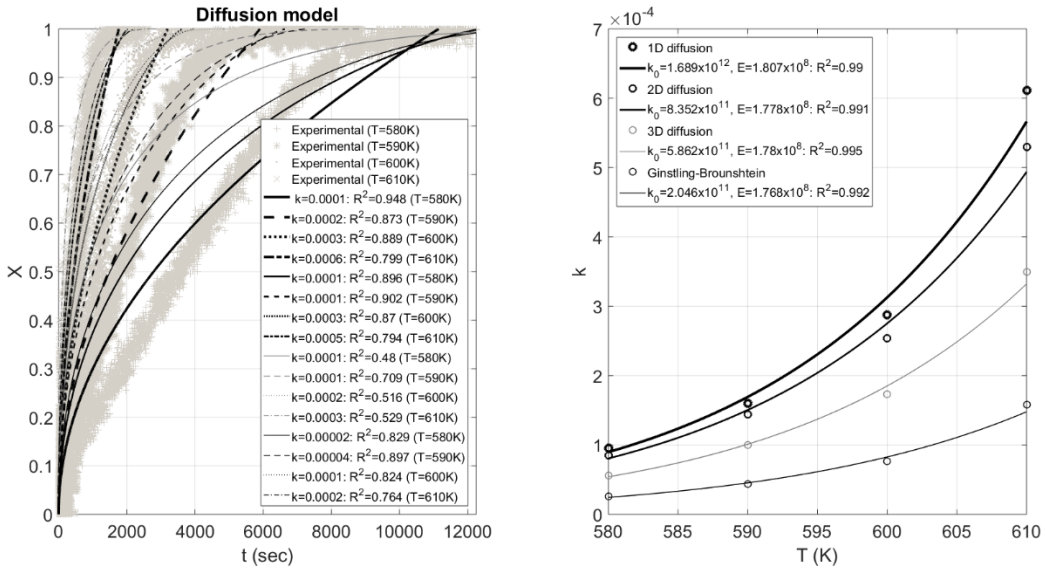



**Figure 5.** The alignment of diffusion models with experimental data at different temperatures, along with fitted curves for the rate constant (k), follows the principles of the Arrhenius equation.

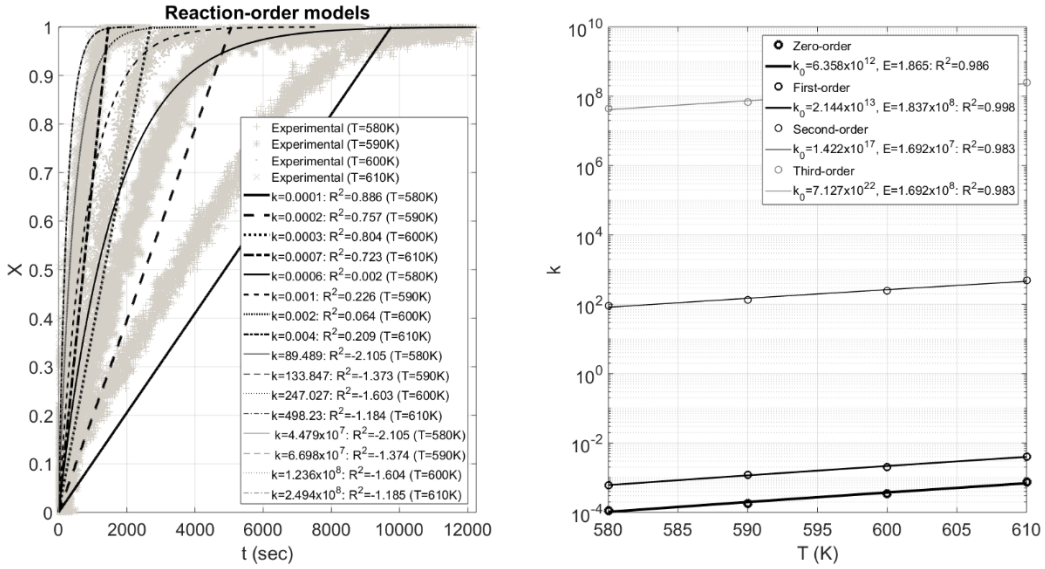



**Figure 6.** The alignment of reaction-order models with experimental data at different temperatures, along with fitted curves for the rate constant (k), follows the principles of the Arrhenius equation.

A comparative inspection of Figures 1 to 6 further elucidates the mechanistic evolution of cellulose degradation across the conversion range. The power-law models (Figure 1) exhibit good agreement with experimental data primarily at the initial stages of conversion, indicating that early degradation is influenced by surface-initiated reactions where the reaction rate scales with fractional conversion. However, their predictive capability diminishes as conversion progresses, reflecting their inability to capture evolving particle geometry.

The Avrami–Erofe'ev and nucleation-and-growth models (Figures 2 and 3) show reasonable fits over limited conversion intervals, particularly toward intermediate and final stages, suggesting localized nucleation effects associated with structural rearrangement or secondary decomposition of residual cellulose. Nonetheless, the additional fitting parameter required for these models introduces uncertainty and reduces their robustness when compared to simpler geometric formulations.

In contrast, the geometrical contraction models presented in Figure 4 provide consistently high-quality fits throughout the majority of the degradation process. This behavior confirms that cellulose decomposition proceeds via a shrinking-core-type mechanism, where rapid nucleation at the particle surface is followed by inward propagation of the reaction interface. The comparable performance of contracting area and contracting volume models reflects the irregular morphology of the cellulose particles, which cannot be idealized as perfectly spherical or cylindrical.

Diffusion-controlled models (Figure 5) display acceptable fits only in limited conversion domains, indicating that internal mass transfer resistance does not govern the overall reaction rate under the selected experimental conditions. Finally, reaction-order models (Figure 6) fail to reproduce the experimental trends adequately, reinforcing the conclusion that cellulose degradation is a heterogeneous, interface-controlled process rather than a homogeneous kinetic reaction.

According to the Geometrical Contraction models, nucleation takes place rapidly on the surface of the crystal. The advancement of the reaction interface towards the crystal's center is governed by the degradation rate. The optimal model for the contracting area indicates that solid particles tend to adopt cylindrical forms rather than spherical or cubical ones [24]. Various mathematical models can be formulated based on these observations. If one considers a solid particle to be either spherical, cubical, or cylindrical (as illustrated in Figure 4), it can be derived from models representing a contracting cylinder (for contracting area) or a contracting sphere/cube (for contracting volume).

The solid material exhibits heterogeneity, and the high $R^2$ values observed in several models, including power law, Avrami-Erofe'ev, contracting, and diffusion, suggest that various models are effective at different stages of the reaction. Analysis of the data points in relation to the fitted lines (as illustrated in Figures 1-6) indicates that the power law model is particularly effective at the onset of the reaction. In contrast, geometrical models, which account for the influence of surface area, play a significant role throughout the majority of the reaction duration. Meanwhile, the Avrami-Erofe'ev and nucleation models are primarily influential towards the conclusion of the reaction period. However, it is noteworthy that the reaction order models did not align well with the experimental data.

The volume contraction mechanism associated with this degradation phenomenon suggests a value of $E$=1.795×$10^8$ J/kmol (refer to Figure 4), which aligns closely with the values derived from alternative models (as illustrated in Figures 1 to 6) and demonstrates an acceptable $R^2$ mean as presented in Table 1.

ARTICLE IN PRESS

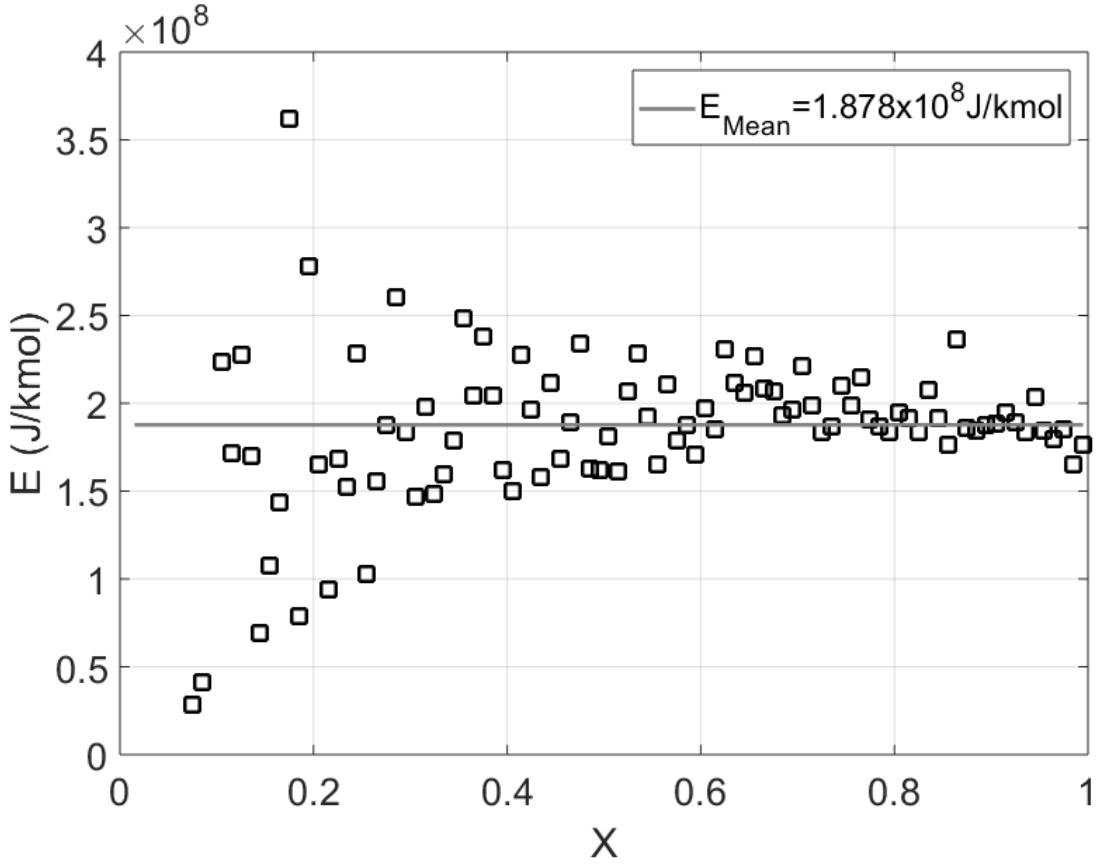



**Figure 7.** The assessment of activation energy associated with the degradation of cellulose through a model-free approach.

Figure 7 illustrates the relationship between activation energy and the extent of degradation progression, as determined by the model-free approach. This figure reveals that the average activation energies obtained are remarkably similar to the values calculated using the established models presented in Table 1. The analysis of activation energy ($E_a$) as a function of the extent of conversion (α), derived from the model-free (iso-conversional) method and presented in Figure 7, provides critical insights into the homogeneity of the degradation mechanism. The near-constant $E_a$ profile observed across the primary conversion range (approximately α=0.1 to α=0.8) strongly suggests that the thermal decomposition of cellulose proceeds predominantly via a single, rate-limiting reaction mechanism. This finding robustly corroborates the results from the model-fitting approach, which identified the geometric contraction models as providing the best statistical fit. The consistency in $E_a$ confirms that the rate-controlling step, the receding reaction interface, remains dominant throughout the bulk of the thermal process, validating the proposed reliance on interfacial area reduction. The subtle, slight increase in $E_a$ observed toward the very final stages of conversion (α>0.9) may signal a minor shift in the controlling kinetics, likely reflecting the decomposition of thermally stable intermediate products or the degradation of highly crystalline cellulose fractions, which typically involve marginally higher energy barriers. The discrepancies observed in the calculated activation energy at varying degrees of degradation can be attributed to the inherent complexity of the phenomenon under investigation, as well as the tolerances present within the experimental setup. Minor fluctuations in this value are primarily due to the tolerances of the experimental system, while significant variations suggest alterations in the underlying degradation mechanisms [18, 19].

ARTICLE IN

The activation energy for cellulose degradation determined here (1.75–2.79 × $10^8$ J·kmol$^{-1}$) shows relatively low variability, suggesting a consistent decomposition pathway under the studied conditions. Comparing this with other biomass constituents highlights distinct behavioral differences. Hemicellulose typically exhibits activation energies in a lower range (e.g., 1.32–1.86 × $10^8$ J·kmol$^{-1}$) but often with greater data scatter. Lignin is known for its highly variable reported activation energies (e.g., 6.2–2.71 × $10^8$ J·kmol$^{-1}$), reflecting its heterogeneous and complex aromatic structure, which leads to diverse decomposition pathways. Such variations across studies can also arise from differences in biomass sources, sample preparation, and kinetic analysis methods [25, 26].

The activation energy range obtained in this study (1.75–2.79 × $10^8$ J·kmol$^{-1}$) is consistent with values reported in the literature for cellulose degradation under inert conditions. For example, Dahiya et al. [12] reported activation energies between 1.6 and 2.5 × $10^8$ J·kmol$^{-1}$ using combined isothermal and non-isothermal analyses. More recently, Li et al. [13] reported values in the range of 1.8–2.6 × $10^8$ J·kmol$^{-1}$ using advanced iso-conversional methods.

In addition, Martínez et al. [16] demonstrated that isothermal kinetic analyses tend to yield narrower activation energy distributions compared to non-isothermal methods, supporting the relatively low variability observed in the present study. The dominance of surface-controlled mechanisms reported here is also consistent with recent findings emphasizing the role of reaction interface reduction in cellulose pyrolysis [14, 15]. These agreements confirm that the experimental data and kinetic interpretations presented in this work are both reliable and representative of intrinsic cellulose degradation behavior.

## 5. Conclusions

In this study, the thermal degradation behavior of cellulose was systematically examined under strictly isothermal conditions using thermogravimetric analysis, with the aim of identifying the intrinsic degradation mechanism and establishing reliable kinetic parameters. Unlike many previous studies that rely on non-isothermal heating programs and broad temperature ranges, the present investigation employed a narrow temperature window (580–610 K), allowing the degradation process to be analyzed with minimal interference from heat and mass transfer limitations.

The kinetic evaluation demonstrated that cellulose degradation under the investigated conditions is best described by geometric contraction mechanisms, indicating that the reaction rate is controlled by the progressive reduction of the reactive interface as degradation proceeds inward from the particle surface. This finding confirms that cellulose decomposition is fundamentally a heterogeneous, surface-controlled process, rather than one governed by homogeneous reaction order kinetics or bulk diffusion phenomena. The observed transition in model applicability across the conversion range further reflects the structural heterogeneity of cellulose, where surface-initiated reactions dominate early stages and interface-controlled behavior persists through most of the degradation process.

The apparent activation energy obtained from both model-fitting and model-free analyses exhibited a relatively narrow range (1.75–2.79 × $10^8$ J·kmol$^{-1}$), supporting the presence of a single dominant rate-limiting mechanism over the majority of conversion. The close agreement between these two independent approaches strengthens the reliability of the derived kinetic parameters and confirms that the isothermal experimental design effectively captures intrinsic

ARTICLE IN PRESS

chemical kinetics. Moreover, the activation energy values are consistent with recent literature reports for cellulose degradation under inert atmospheres, further validating the experimental methodology and analytical framework.

A key outcome of this study is the development of a predictive kinetic expression capable of describing cellulose degradation under controlled isothermal conditions. This kinetic formulation provides a practical basis for modeling cellulose behavior in applications such as biomass pyrolysis, energy conversion systems, fire-retardant material design, and thermal stability assessment of cellulose-based composites. By emphasizing mechanism identification rather than sole reliance on activation energy estimation, this work contributes to a more physically meaningful understanding of cellulose thermal decomposition. Ultimately, an equation was derived to forecast the progression of cellulose degradation:

$$1-(1-X)^{\frac{1}{3}} = 1.017 \times 10^{12}\, e^{\frac{-1.795\times10^{8}}{RT}} t \quad (5)$$

Future studies should extend this mechanistic approach to different cellulose sources, particle morphologies, and chemically modified systems, as well as to multicomponent lignocellulosic materials. Such investigations will further enhance the predictive capability of kinetic models and support the optimization of sustainable biomass-based technologies.

**Acknowledgements**

This research received partial support from Aseman Laal Fam (www.Alfaunity.com). We express our gratitude to our colleagues at Alfaunity for their valuable insights and expertise, which significantly contributed to the research.

**Nomenclature**

| **Symbols** | | **Abbreviation** | |
|---|---|---|---|
| $T$ | Absolute temperature (K) | TGA | Thermogravimetric analysis |
| $t$ | Time (s or min) | TGA–FTIR | Combined thermogravimetric analysis–Fourier transform infrared spectroscopy |
| $\alpha$ | Degree of conversion (fractional mass loss) | K | Kelvin (unit of absolute temperature) |
| $\alpha_0$ | Initial conversion degree | J·kmol$^{-1}$ | Joule per kilomole (unit of molar activation energy) |
| $\alpha_f$ | Final conversion degree | | |
| $k$ | Rate constant (s$^{-1}$) | | |
| $k_0$ or $A$ | Pre-exponential factor (frequency factor) (s$^{-1}$) | | |
| $E_a$ | Apparent activation energy (J·mol$^{-1}$ or J·kmol$^{-1}$) | | |
| $R$ | Universal gas constant (J·mol$^{-1}$K$^{-1}$ or J·kmol$^{-1}$·K$^{-1}$ (consistent with $E_a$)) | | |
| $d\alpha/dt$ | Reaction rate (conversion rate) (s$^{-1}$) | | |
| $m$, $m_0$, $m_t$, | Sample mass, initial mass, mass at time t (g or mg) | | |
| $\beta$ | Heating rate (for non-isothermal experiments, if used) (K·min$^{-1}$ or K·s$^{-1}$) | | |
| $n$ | Reaction order / power-law exponent | | |
| $f(\alpha)$ | Differential conversion function in kinetic model | | |
| $g(\alpha)$ | Integral conversion function in kinetic model | | |

ARTICLE IN PRESS

## References

[1] Leroy, V., Leoni, E., Cancellieri, D., 2010. Thermal degradation of lignocellulosic fuels: biopolymers contribution, In: Elnashar, M. (Ed.), Biopolymers, IntechOpen, London. http://dx.doi.org/10.5772/10267

[2] Burnham, A.K., Zhou, X., Broadbelt, L.J., 2015. Critical review of the global chemical kinetics of cellulose thermal decomposition, Energy & Fuels, 29 (5), 2906-2918. http://dx.doi.org/10.1021/acs.energyfuels.5b00350

[3] Zheng, C., Li, D., Ek, M., 2019. Mechanism and kinetics of thermal degradation of insulating materials developed from cellulose fiber and fire retardants, Journal of Thermal Analysis and Calorimetry, 135 (6), 3015-3027. http://dx.doi.org/10.1007/s10973-018-7564-5

[4] Lazzari, L., Neves, R.M., Vanzetto, A.B., Zattera, A.J., Santana, R.M.C., 2022. Thermal degradation kinetics and lifetime prediction of cellulose biomass cryogels reinforced by its pyrolysis waste, Journal of Materials Research, 37 (13), 2736-2747.

[5] Wanjun, T., Yuwen, L., Hen, Z., Zhiyong, W., Cunxin, W., 2003. New temperature integral approximate formula for non-isothermal kinetic analysis, Journal of Thermal Analysis and Calorimetry, 74 (1), 309-315. http://dx.doi.org/10.1023/A:1026310710529

[6] Roman, M., Winter, W.T., 2004. Effect of sulfate groups from sulfuric acid hydrolysis on the thermal degradation behavior of bacterial cellulose, Biomacromolecules, 5 (5), 1671-1677.

[7] Morooka, T., Norimoto, M., Yamada, T., Shiraishi, N., 1984. Dielectric properties of cellulose acylates, Journal of Applied Polymer Science, 29 (12), 3981-3990. https://doi.org/10.1002/app.1984.070291230

[8] Sealey, J.E., Samaranayake, G., Todd, J.G. and Glasser, W.G., 1996. Novel cellulose derivatives. IV. Preparation and thermal analysis of waxy esters of cellulose, Journal of Polymer Science Part B: Polymer Physics, 34 (9), 1613-1620. https://dx.doi.org/10.1002/(SICI)1099-0488(19960715)34:9<1613::AID-POLB10>3.0.CO;2-A

[9] Signori-Iamin, G., Aguado, R.J., Tarrés, Q., Mutjé, P. and Delgado-Aguilar, M., 2025. Chemical Modification of Cellulose. In The Handbook of Paper-Based Sensors and Devices: Volume 1: Materials and Technologies (pp. 153-182). Cham: Springer Nature Switzerland.

[10] Huang, M.R. and Li, X.G., 1998. Thermal degradation of cellulose and cellulose esters. Journal of applied polymer science, 68(2), pp.293-304.

[11] Huang, F.Y., 2012. Thermal properties and thermal degradation of cellulose tri-stearate (CTs). Polymers, 4(2), pp.1012-1024.http://dx.doi.org/10.3390/polym4021012

[12] Dahiya, J.B., Kumar, K., Muller-Hagedorn, M. and Bockhorn, H., 2008. Kinetics of isothermal and non-isothermal degradation of cellulose: model-based and model-free methods. Polymer International, 57(5), pp.722-729.

[13] Dobrovská, J., Skalková, P., Drozdová, L., Labaj, I., Zlá, S., Dubec, A. and Kawuloková, M., 2024. Pyrolysis of natural rubber–cellulose composites: isoconversional kinetic analysis based on thermogravimetric data. Journal of Thermal Analysis and Calorimetry, 149(8), pp.3111-3124.

[14] Kim, U.J., Eom, S.H. and Wada, M., 2010. Thermal decomposition of native cellulose: influence on crystallite size. polymer degradation and stability, 95(5), pp.778-781.

[15] Saha, S., Phadke, P., Chowdhury, A. and Kumbhakarna, N., 2025. Understanding the mechanism of Guanidinium nitrate decomposition–A TGA-FTIR, temperature-jump/FTIR and laser pyrolysis/FTIR study. Thermochimica Acta, 751, p.180059.

[16] Annapureddy, P.K.R., Ranjan, A. and Kishore, N., 2025. Kinetics, reaction models, and thermodynamic feasibility of non-isothermal catalytic pyrolysis of Erythrina indica. Journal of Renewable and Sustainable Energy, 17(2).

[17] Vasudev, V., Ku, X., Ram, S., Memon, T.A., Patil, Y., Shoaib, M., Liu, Z. and Wang, Z., 2025. An exploration of strategies for conducting kinetic analysis of lignocellulosic and algal biomass pyrolysis. BioEnergy Research, 18(1), p.64.

[18] Abolpour, B., Afsahi, M.M., Azizkarimi, M., 2021. Hydrogen reduction of magnetite concentrate particles, Mineral Processing and Extractive Metallurgy, 130 (1), 59-72.

[19] Abolpour, B., Afsahi, M.M., Azizkarimi, M., 2018. Reduction kinetics of magnetite concentrate particles by carbon monoxide, Mineral Processing and Extractive Metallurgy, 127 (1), 29-39.

ARTICLE IN PRESS

[20] Abolpour, B., Shamsoddini, R., 2020. Mechanism of reaction of silica and carbon for producing silicon carbide, Progress in Reaction Kinetics and Mechanism, 45 (1), 74-88. http://dx.doi.org/10.1177/1468678319891416

[21] Pourghahramani, P., Forssberg, E., 2007. Reduction kinetics of mechanically activated hematite concentrate with hydrogen gas using nonisothermal methods, Thermochimica Acta, 454 (2), 69-77.

[22] Abolpour, B., 2021. A numerical study of the volume oxidation of $UO_2$ pellets in the oxidation process, Oxidation of Metals, 95 (1-2), 1-16. http://dx.doi.org/10.1007/s11085-020-10012-6

[23] Fedunik-Hofman, L., Bayon, A., Donne, S.W., 2019. Kinetics of solid-gas reactions and their application to carbonate looping systems, Energies, 12 (15), 2981. http://dx.doi.org/10.3390/en12152981

[24] Khawam, A., Flanagan, D.R., 2006. Solid-state kinetic models: basics and mathematical fundamentals, Journal of Physical Chemistry B, 110 (35), 17315-17328. http://dx.doi.org/10.1021/jp062746a

[25] Zhang, J., Chen, T., Wu, J., Wu, J., 2014. Multi-Gaussian-DAEM-reaction model for thermal decompositions of cellulose, hemicellulose and lignin: comparison of $N_2$ and $CO_2$ atmosphere, Bioresource Technology, 168, 87-95.

[26] Gomez, I.J., Arnaiz, B., Cacioppo, M., Arcudi, F., Prato, M., 2018. Nitrogen-doped carbon nanodots for bioimaging and delivery of paclitaxel, Journal of Materials Chemistry B, 6 (4), 554-562. http://dx.doi.org/10.1039/C8TB01796D

ARTICLE IN PRESS